Turkey oak (*Quercus cerris* L.) is more drought tolerant and better reflects climate variations compared to pedunculate oak (*Quercus robur* L.) in lowland mixed forests in northwestern Serbia: A stable carbon isotope ratio (δ13C) and radial growth approach

Saša Kostić [a,1], Tom Levanič [b,*,2], Saša Orlović [a,3], Bratislav Matović [a,4], Dejan B. Stojanović [a,5]

[a] *Institute of Lowland Forestry and Environment, University of Novi Sad, Antona Čehova 13d, 21000 Novi Sad, Serbia*
[b] *Slovenian Forestry Institute, Večna pot 2, 1000 Ljubljana, Slovenia and University of Primorska, Faculty of Mathematics, Natural Sciences and Information Technologies, Glagoljaška 8, SI-6000 Koper, Slovenia*

ABSTRACT

Tree-ring width (TRW), stable carbon isotope ratio (δ^{13}C) and intrinsic water use efficiency (iWUE) data set chronologies were built for the period 1961–2000 for two oak species (pedunculate oak – *Quercus robur* L. and Turkey oak – *Quercus cerris* L.) in northwestern Serbia (Vojvodina province). We focused on the response of the two oak species to measured meteorological data (temperature, precipitation and cloud cover), drought events expressed by six meteorological drought indices, and river water level to better understand their drought tolerance and stress and to assess the reliability of the species response to climate and drought indices when using TRW or δ^{13}C. Turkey oak exhibited better drought tolerance (and less drought stress) compared to pedunculate oak, as manifested, respectively, by less negative δ^{13}C and lower iWUE values. Based on a generalised additive mixed model (GAMM) among the six drought indices studied, the standardised precipitation evapotranspiration index and the standardised precipitation index showed the best fit with both TRW and δ^{13}C, while the Palmer drought severity index exerted a strong influence only on TRW. It was thus concluded that δ^{13}C responds more strongly and rapidly to climate variations than TRW.

1. Introduction

Climate variability is significantly affecting forests around the world (Bugmann and Pfister, 2000; Hoffmann et al., 2018; McDowell et al., 2020). Climate change (global warming and a degraded hydrological cycle) since the 1950 s has led to more extreme drought events (IPCC, 2019) and to increased forest mortality (Keenan, 2015; Alexandrov and Iliev, 2019; Losseau et al., 2020).

Three oak decline waves and mortality events (1983–1987, 2014 and 2018) have been observed across Europe since 1960 (Haavik et al., 2015; Neuwirth et al., 2021). Severe drought periods caused similar

waves of oak decline in Serbia in 1983–1986, 2010–2013 and 2017 (Stojanović et al., 2015; Kostić et al., 2021c). Intensifying climate change led to a significant decline in the radial growth of pedunculate oak (*Quercus robur* L.) throughout Europe in the 20th and 21st centuries. These declining trends have also been noted in the 2500-year tree-ring width chronology of pedunculate oak (Büntgen et al., 2011) and in studies of this species covering shorter time spans from the Pannonian Plain (Levanič et al., 2011; Stojanović et al., 2015; Arvai et al., 2018) and wider geographical region (Voelker et al., 2014; Losseau et al., 2020).

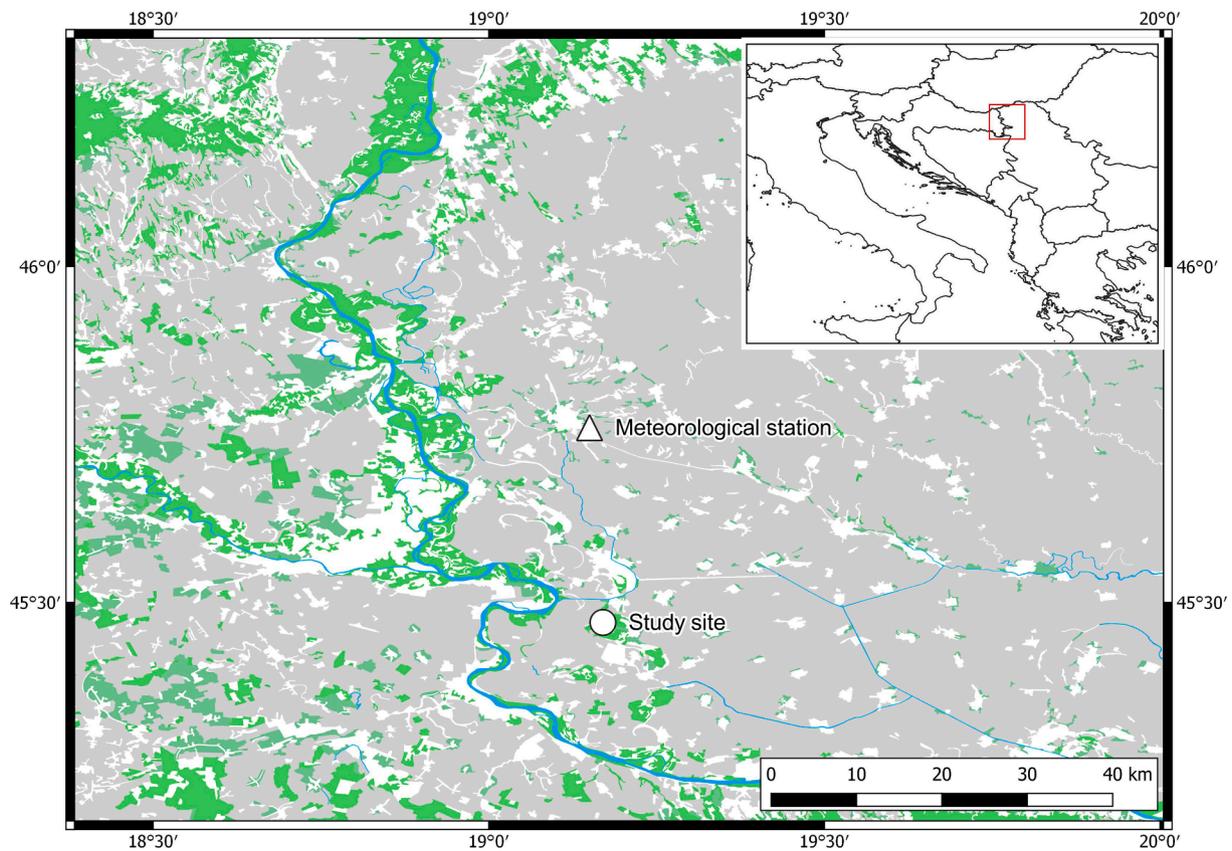Drought is recognized as an important driver of forest mortality

Fig. 1. Map of the study area in NW Serbia with the location of the study area in the wider geographical context.

(Allen et al., 2010) as it can cause significant changes in the structure and function of forest ecosystems (Assal, Anderson, and Sibold, 2016). Furthermore, the radial growth responses of trees to drought are complex due to simultaneous exposure to multiple environmental stressors (Huang et al., 2018; Kostić et al., 2021c). Nevertheless, most authors agree that such responses are determined by tree characteristics, e.g. genetics, age, fitness and tree architecture, as well as by surrounding environmental factors, e.g. soil properties, climatic conditions, water regime, stand mixture and density (Pretzsch, 2009), and are amplified by intense climate change (McDowell et al., 2020). The sensitivity of the radial increment has been investigated using (i) measured climate data such as temperature, precipitation, sunshine and cloud cover (Huang et al., 2018; Zheng et al., 2019); (ii) drought events (Timofeeva et al., 2017; Hoffmann et al., 2018; Kostić et al., 2021b); (iii) soil moisture (Kostić et al., 2021b); (iv) river water levels (Stojanović et al., 2015; Skiadaresis et al., 2019; Netsvetov et al., 2019; Gholami et al., 2021); and (v) biotic stressors (Csank et al., 2016; Losseau et al., 2020).

The sensitivity of the annual radial increment of pedunculate oak to climate and environmental factors has been widely studied (see Büntgen et al., 2011; Levanič et al., 2011; Hafner et al., 2015; Nechita et al., 2018; Stojanović et al., 2018; Landi et al., 2019; Losseau et al., 2020; Kostić et al., 2021b, 2021c), while the broader use of stable carbon ($\delta^{13}C$), hydrogen (δ^2H) and oxygen ($\delta^{18}O$) isotopes to study the response of oaks to environmental factors has only recently emerged. Recent studies have shown that stable isotopes in oaks may be a better indicator of tree response to climate and environmental factors than tree-ring widths (Loader et al., 2008; Hafner et al., 2011; Loader et al., 2019, Büntgen et al., 2020). Stable carbon isotope ratios also show a faster and earlier response to climate and environmental factors (Hafner et al., 2011) than tree-ring widths, which have a prolonged effect of up to three years (Stojanović et al., 2018).

Stomatal conductance and the amount of CO_2 in the intercellular space are important in the process of ^{13}C sequestration trough the Calvin cycle into the tree metabolism, and finally its incorporation into the wood cellulose (Farquhar et al., 1989). If the stomata are open, biological processes in the leaves tend to use ^{12}C in preference to ^{13}C, which happens when the stomata are closed. In hot and dry years when the stomata are often closed and trees are struggling to find water, the ratio of stable carbon isotope will be in favour of ^{13}C and their ratio in the wood α-cellulose will be less negative (McCarroll and Loader, 2004, Loader et al., 2008).

Species-specific responses to drought further complicate the understanding of drought-induced changes in forests (Adams et al., 2017; Zheng et al., 2019). Therefore, further studies are needed, especially those focusing on endangered and economically important tree species and their vulnerable southern marginal populations under changing climate conditions (Annighöfer et al., 2015), such as the two oak species examined in our study. The analysed $\delta^{13}C$ values and radial growth patterns should foster a deeper understanding of tree adaptation to new, changing climate conditions and extreme drought events in the coming period (McDowell et al., 2008; Schnabel et al., 2022).

1.1. Objectives and questions of this study

The two analysed oak species are widespread in Pannonian lowland forests in northwestern (or NW) Serbia. They are economically important and sensitive to warming and ongoing intensive climate change. We used (i) tree-ring widths (TRW), (ii) stable carbon isotope ratio ($\delta^{13}C$) and (iii) intrinsic water use efficiency (iWUE) data to study growth dependence and physiological responses to changing climate with a focus on drought events. For the latter we calculated six different meteorological drought indices given that not all drought indices are suitable for studying plant sensitivity to drought.

Our main goal was to gain a better understanding of the response of pedunculate oak and Turkey oak to drought as well as of differences in the TRW, $\delta^{13}C$ and iWUE response of the analysed oaks to climate and
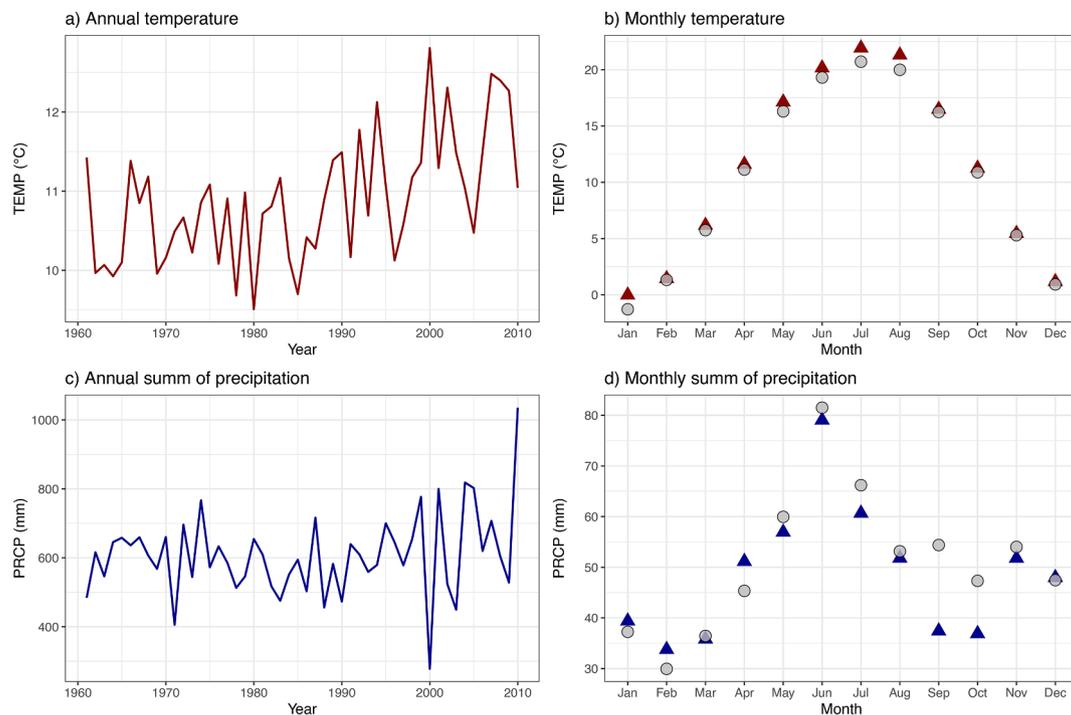
Fig. 2. First (1961–90, ● mark) and last 30 year (1981–2010, ▲ mark) time span mean values of TEMP – red lines (°C) and annual PCPT – blue lines (mm m^{-2}), with month (**a, c**) and year (**b, d**) as grouping variables. (For interpretation of the references to colour in this figure legend, the reader is referred to the web version of this article.)

environmental changes. Additionally, we sought to address the following questions:

(i) Are differences in TRW, δ^{13}C and iWUE chronologies between pedunculate oak (*Quercus robur* L.) and Turkey oak (*Quercus cerris* L.) caused by species-specific characteristics?

(ii) Are meteorological drought indices reliable indicators of TRW and δ^{13}C variations?

(iii) Does the δ^{13}C and TRW of a more drought-tolerant oak species better reflect surrounding climate events?

2. Materials and methods

2.1. Study area and data description

TRW chronologies were obtained from a 480 ha even-aged mixed lowland forest complex located in NW Serbia (Vojvodina Province). The site is located ~ 5 km from the Danube River, the largest river basin in SE Europe (45° 28′ N and 19° 10′ E; elevation: 80 m a.s.l.). Due to the lowland character of the area, the ecological conditions are almost identical across the entire studied forest stand (Fig. 1). The soil can be characterized as Solonetz, which is a slightly saline, holomorphic and poor soil type (described in more detail in Kostić et al., 2021a).

The main tree species at the studied site are pedunculate oak (*Quercus robur* L.; QURO) and Turkey oak (*Quercus cerris* L.; QUCE), with a small share of *Fraxinus* sp. and *Carpinus* sp. in the understory. Only vital, dominant or co-dominant (1 and 2 after Kraft classification (Kramer 1988)) QURO and QUCE with no visible trunk damage were included in the sample. The selected trees were approximately 120 years old.

A total of 20 (10 QURO and 10 QUCE) stem discs were collected in 2013 and 2014 and used to create the same number of TRW series. Twelve of the 20 (6 QURO and 6 QUCE) stem discs were selected to determine δ^{13}C in tree rings over a 50-year period (1961–2010). Each tree TRW series was constructed from two opposing directions of the stem disc. TRW analyses were performed at the dendrochronological

laboratory of the Institute of Lowland Forestry and Environment (Serbia), while δ^{13}C analyses were carried out at the Stable Isotope Laboratory of the Slovenian Forestry Institute (Slovenia).

2.2. Tree-ring widths, stable carbon isotope and intrinsic water use efficiency analyses

For the TRW analysis, sampled stem discs were dried and sanded with progressively higher grit sand paper to achieve a highly polished surface for measuring purposes. Stem discs were then scanned with an ATRICS high-resolution image capturing system (Levanič, 2007) and tree-ring widths were measured using WinDENDRO software. Measured TRWs were imported into PAST-5^{TM} dendrochronological software for cross-checking, dating and synchronization. The same sample preparation procedure was used for the stable isotope analysis samples, except that chalk was not used to improve tree-ring visibility and grinding dust was removed with an oil-free air compressor. In addition, all TRWs were measured and each tree ring was dated to enable the dated tree rings to be later used for cellulose extraction and stable isotope ratio determination.

Alpha-cellulose from the latewood of each tree-ring was obtained following the extraction procedure proposed by Loader et al. (1997). The α-cellulose from each tree ring was then homogenised using a Hielscher ultrasonic homogeniser and freeze-dried in a vacuum at −90 °C for 48 h. Samples of about 350 µg were eventually weighted into tin capsules and packed for stable isotope ratio analysis using an ISO-PRIME 100 (Isoprime, UK) stable isotope ratio mass spectrometer (IRMS) in continuous flow mode connected to a Vario PYRO cube elemental analyser (Elementar GmbH, Germany) running in combustion mode at the Stable Isotope Laboratory of the Slovenian Forestry Institute, Ljubljana (Slovenia).

Raw stable carbon isotope ratio data were corrected for changing δ^{13}C values in the atmosphere using the so-called "atmospheric correction" (see McCarroll and Loader, 2004). After approximately CE 1850, δ^{13}C values of atmospheric CO_2 decreased, primarily due to the burning of fossil fuels that are depleted in δ^{13}C. This "atmospheric decline'' is
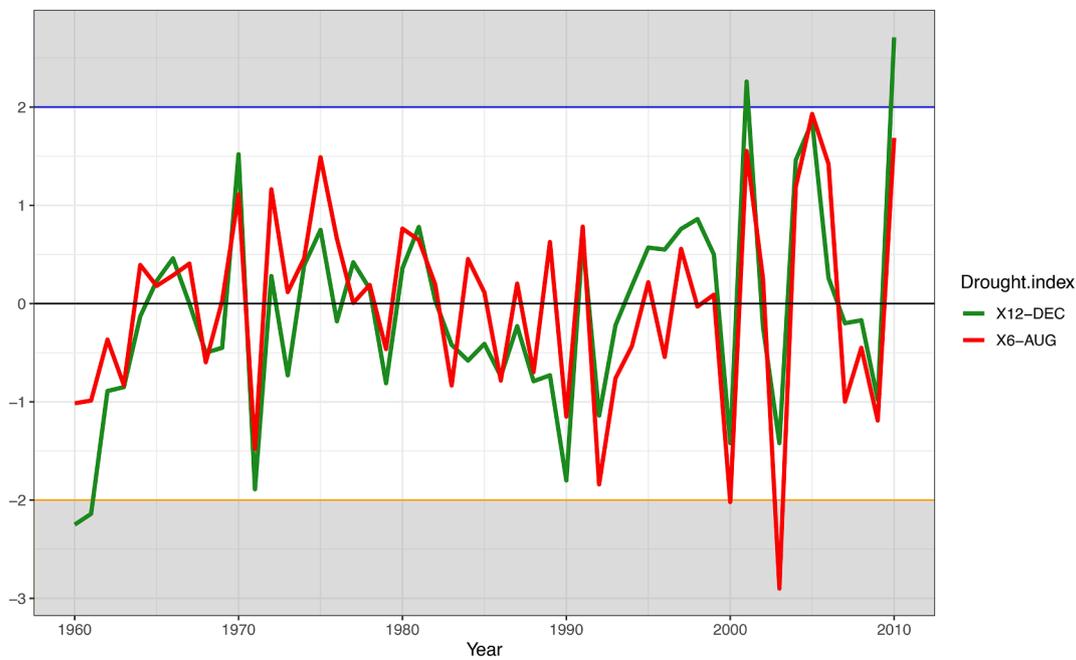
Fig. 3. Combined drought indices for the vegetation period (March-August) marked as X_6 and for the annual level marked as X_{12}, for the 1960–2010 time span.

directly reflected in tree-ring $\delta^{13}C$ values and is corrected by simply adding to each year the difference between the atmospheric $\delta^{13}C$ value estimated from ice cores or air samples and the estimated value in CE 1850 (-6.4 %). The procedure is described by McCarroll and Loader (2004) and involves a simple mathematical correction to express each $\delta^{13}C$ value relative to the pre-industrial atmospheric $\delta^{13}C$ level. In this way a corrected $\delta^{13}C$ chronology was obtained.

The interpreted $\delta^{13}C$ represents the ratio of lighter (^{12}C) and heavier (^{13}C) carbon stable isotopes by their atmospheric concentration, which was measured and calculated using Eq. (1):

$$\delta_{13}C(‰) = \left(\frac{_{13}C/_{12}C_{sample}}{_{13}C/_{12}C_{standard}} \right) \times 1000 \qquad (1)$$

where $^{13}C/^{12}C_{standard}$ is the Vienna PeeDee Belemnite (V-PDB) standardized coefficient (Farquhar et al., 1989) and $^{13}C/^{12}C_{sample}$ is the measured value (Farquhar et al., 1989; Saurer and Siegwolf, 2007). All values of stable isotope ratios are expressed in per-mill notation (‰).

Intrinsic water use efficiency (iWUE) relates to water loss via the stomata (stomatal conductance) and net CO_2 assimilation (A/g_s). The iWUE can be derived from $\delta^{13}C$ using Eq. (2) (Farquhar et al., 1982; 1989):

$$iWUE = A/g_s = c_a \times \frac{\left[b - \left(\delta^{13}C_{atm} - \delta^{13}C_{plant} \right) \right]}{\left[(b - a) \times 1.6 \right]} \qquad (2)$$

where c_a is the atmospheric CO_2 concentration, $\delta^{13}C_{atm}$ the stable carbon isotope ratio of atmospheric CO_2, $\delta^{13}C_{plant}$ the stable isotope ratio of the plant, coefficient a (≈ -4.4 ‰) the fractionation due to diffusion, and coefficient b (≈ -27 ‰) the biochemical fractionation.

2.3. Climate data

Daily climate data were taken from the E-OBS gridded database (version 23.1e; source: Copernicus: European Union's Earth observation programme; Cornes et al., 2018). While designing the experiment, we compared the meteorological data (temperature and precipitation) measured at the closest meteorological station at Sombor (45° 46′ N, 19° 09′ E; ~35 km distance from the analysed stand) and the gridded E-OBS data. With the use of Kendall's Tau test, we observed high synchronicity between the measured and gridded time series. Hence, we chose the E-

OBS meteorological dataset, which includes extra meteorological parameters such as solar radiation and cloudiness.

In total, we used ten parameters: nine meteorological parameters and one for river water level (RWL). Daily observations of RWL were taken from the closest measurement station of the Hydrometeorological Service of the Republic of Serbia on the Danube River. Out of the nine meteorological parameters, three were direct measurements, while six were calculated indices. To interpret climate oscillation in a 50-year-long period, we used mean annual temperature (TEMP) and total annual sum of precipitation (PCPT), which were presented as two 30-year means (1961–1990 and 1981–2010); see Fig. 2.

Of the six drought indices, four were calculated at the annual level. The two remaining drought indices, the standardized precipitation index (SPI) and the standardized precipitation evapotranspiration index (SPEI), were calculated at two scales. We chose 6- and 12-month time scales because the time periods mentioned cover the growing season (6-month time scale) and the entire year of tree-ring formation (12-month time scale).

Following the methodology by Spinoni et al. (2015), the combined drought indices for the March-August period (marked as X_6) and December-December period (December of the year preceding tree-ring formation to December of the year of tree-ring formation, marked as X_{12}) were calculated as the average value of SPI and SPEI data for 6- and 12-month accumulation periods at the monthly level. X_6 and X_{12} were used to summarize drought events in their visual interpretation and with TRW and $\delta^{13}C$ data (see Figs. 2 and 3). The SPI is a widely used meteorological drought index based on precipitation data introduced by McKee et al. (1993). The SPI was further upgraded to the SPEI, which takes into account both precipitation and potential evapotranspiration (PET) as a measure of drought severity (Vicente-Serrano et al., 2010).

Four drought indices were calculated at an annual level: the Palmer drought severity index (PDSI), aridity index (AI), forest aridity index (FAI) and potential evaporation (PE). The PDSI was one of the first meteorological drought indices developed by Palmer (1965) and is still widely used around the world. Primarily, PDSI is used for agriculture, but over time, it has been evaluated and used for other natural systems, such as forests. AI was defined by De Martonne (1925) and represents the ratio of the annual sum of precipitation and average temperature. It classifies stand type from semi-humid to excessively-humid. FAI (Führer
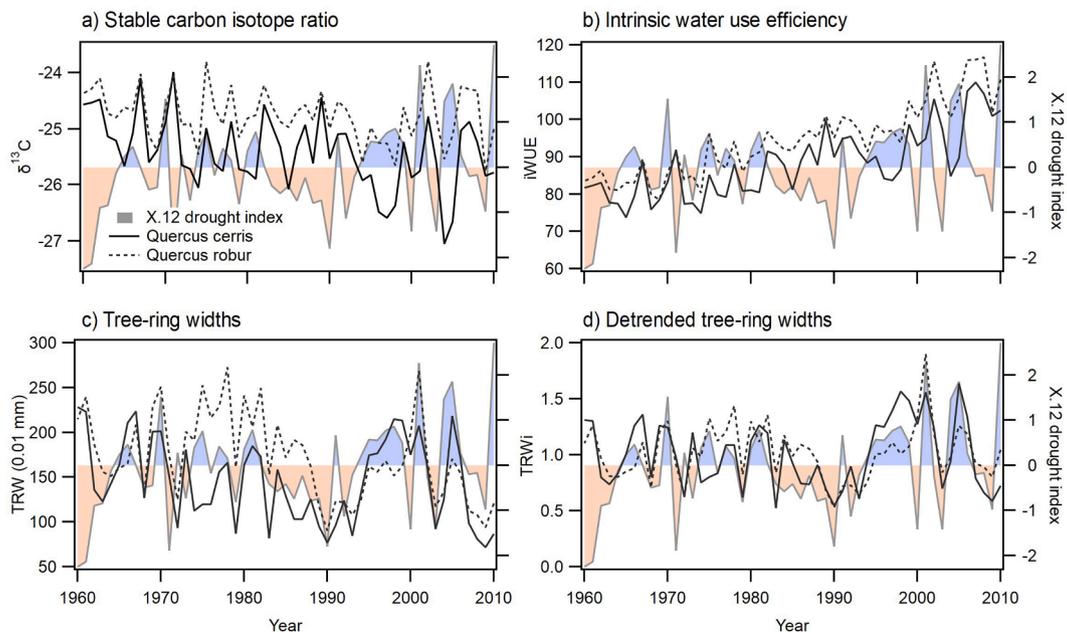
Fig. 4. Comparison of TM^{13}C (**a**), iWUE (**b**), TRW (**c**) and TRWi (**d**) for *Quercus cerris* (solid line) and *Quercus robur* (dotted line) with X$_{12}$ drought index for December (red coloured area represents dry periods, and blue, wet periods). (For interpretation of the references to colour in this figure legend, the reader is referred to the web version of this article.)

et al., 2011) is an aridity index specially designed for forest stands. FAI is calculated using temperature and precipitation data and used to define optimal stand conditions for beach and oak stands. Values lower than 4.75 are classified as beech stands and values between 4.75 and 7.25 as oak stands. The last drought index is PE (Thornthwaite, 1948), which is defined as the hypothetical surface of green grass that is of uniform height, actively growing and adequately watered. It is easily calculated and widely used in biometeorology.

2.4. Statistical data processing

All statistical analyses were performed in R (R Core Team, 2013). TRW chronologies were single detrended using the "modified negative exponential curve" (Fritts, 2001) available in the dplR package (R package developed specifically for dendrochronology, version 1.7.1.; Bunn, 2008). Detrended chronologies were then trimmed to the same time span as meteorological data and drought indices and correlated with the monthly values of the gridded meteorological measurements and drought indices for the analysed 50-year time span (1961–2010). Interactions between detrended TRW (TRWi), δ^{13}C, iWUE and river water level; meteorological measurements; and drought indices were analysed using a generalized additive mixed model (GAMM). For data visualization, the *ggplot2* R package was used (version 3.2.0.; Wickham, 2016).

In the comparative analysis we took QUCE growth as a reference for QURO growth. Inter-species differences (QURO-QUCE$_{IDS}$) were calculated using Eq. 3: $QURO - QUCE_{IDS} = \frac{QURO}{QUCE}$. Synchronicity between QURO and QUCE TRW, δ^{13}C and iWUE chronologies were analysed using Kendall's τcoefficient, via the VGAM R package (Yee, 2010). Kendall's Tau is a non-parametric statistical test which analyses the ordinal association and synchronization between two tested timeseries based on rank correlation. This is a more suitable method for studying dependencies between two time series than parametric tests in tree-ring studies, as shown in Hamed (2011).

2.4.1. Generalized additive mixed model

Given that TRW and other tree-ring properties are affected by surrounding stressors, including nonlinear climate trends, a more flexible

approach to their modelling is required (Wood, 2017). Based on testing both linear and nonlinear models for pedunculate oak from the studied region (Kostić et al., 2021a, 2021b), the GAMM was applied using the mgcv R package (Wood and Wood, 2015; see also Kostić et al., 2021a, 2021b for a detailed explanation of the utilized GAMM and their detailed setup). In the GAMM we used TRWi and the detrended stable carbon isotope ratio (det. δ^{13}C) timeseries to provide the same range and type of time series to the model calculation, as indicated in Eq. (4):

$$\begin{aligned}
Y\ 1 &+ s(PRCP_{MAM}) + s(PRCP_{JJA}) + s(PRCP_{ANNUAL}) + s(TEMP_{MAM}) \\
&+ s(TEMP_{JJA}) + s(TEMP_{ANNUAL}) + s(CLOUD_{MAM}) + s(CLOUD_{JJA}) \\
&+ s(CLOUD_{ANNAUL}) + s(RWL_{MAM}) + s(RWL_{JJA}) + s(RWL_{ANNUAL}) \\
&+ s(FAI) + s(PE) + s(AI) + s(PDSI) + s(SPI6_{AUG}) + s(SPI12_{AUG}) \\
&+ s(SPEI6_{AUG}) + s(SPEI12_{AUG}) + (Tree) + CorCAR1(Year|(Tree))
\end{aligned}$$

$$(4)$$

where Y denotes TRWi or det. δ^{13}C. Temperature (TEMP), precipitation (PRCP), cloudiness (CLOUD) and river water level (RWL) were interpreted for 12-month (based on the vegetation period from September of the year prior to tree-ring formation to August of the year of ring formation) and two 3-month periods: March to May (MAM) and June to August (JJA). Drought was entered in the model with six drought indices (FAI, PE, AI, PDSI, SPI and SPEI). The SPI and SPEI were calculated for August with 6- and 12-month accumulation periods. The abbreviations and descriptions of all 20 variables and their sources are provided in Appendix A (see Table A1). The variable "Tree" was used in the GAMM as a random effect.

3. Results

3.1. Site conditions and drought periods in the analysed time span

Climate in the sampling area is defined as temperate continental to modified continental, with semi-humid and warm summers (Kottek et al., 2006). Following a 50-year time span (1961–2010), TEMP was 10.9 °C (JJA 20.6 °C) and PCPT was 682.5 mm (JJA 200.8 mm). In line with the pronounced changes in climate in the 21st century and rapid temperature increase (Ruosteenoja et al., 2018), stand climate
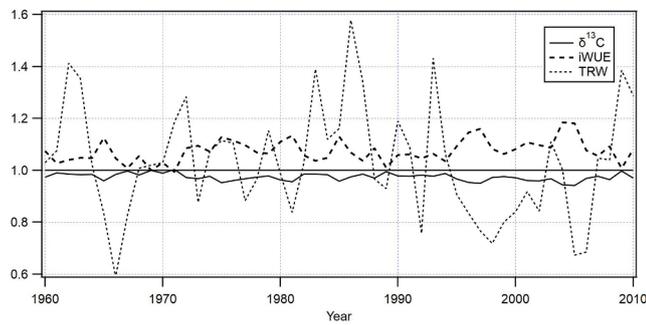
Fig. 5. Inter-species variations expressed as the quotient between QURO and QUCE in TRW (dotted line), TM^{13}C (solid line) and iWUE (dashed line), following Eq. 3.

conditions have changed (see Fig. 2). During the first decades of the 21st century, the temperature was higher by 1.0 to 1.5 °C during the summer months and slightly less during the rest of the year in comparison to the 1961–2000 period.

When comparing average monthly temperature and average sum of precipitation for the 1960–1990 period (Fig. 2; symbol: ●) with the most recent 1981–2010 period (Fig. 2; symbol: ▲), the climate was warmer in the late spring (April, May) and summer months (JJA; Fig. 2b). Precipitation was consistently higher between May and August in the 1961–1990 period than in the 1980–2010 period. The highest precipitation deficit was recorded for September and October of the 1981–2010 period. In the period 1981–2010, drought events were almost constantly present between May and October, which means that trees were under constant drought stress (Fig. 2d). Regarding annual average temperature and sum of precipitation (Fig. 2a and 2c), an increasing number of extreme events was noted in the last two decades (1991–2010) and

Table 1

Generalized additive mixed model (GAMMs; Eq. (4).) outputs for TRWi and det. δ^{13}C for both analysed oaks (*Quercus robur* and *Quercus cerris*) over a 50-year time span (1961–2010).

Pedunculate oak (*Quercus robur* L.)						
	TRWi			**det. δ^{13}C**		
Variable	**EDF**	**F (p)**	**k-index (p)**	**EDF**	**F (p)**	**k-index (p)**
TEMP$_{MAM}$	3.26	6.52*	0.80 ^{NS}	1.51	10.29**	0.98 ^{NS}
TEMP$_{JJA}$	2.02	5.70 ^{NS}	0.73 ^{NS}	1.87	5.33 ^{NS}	0.71 ^{NS}
TEMP$_{ANNUAL}$	1.17	5.49 ^{NS}	0.76 ^{NS}	1.60	5.50 ^{NS}	0.64 ^{NS}
PRCP$_{ANNUAL}$	1.90	7.75**	0.85^{NS}	1.41	6.50 ^{NS}	0.70 ^{NS}
PRCP$_{MAM}$	1.40	7.51**	0.88 ^{NS}	1.32	7.16*	0.78 ^{NS}
PRCP$_{JJA}$	1.00	5.44 ^{NS}	0.83 ^{NS}	3.45	8.98*	0.86 ^{NS}
CLOUD$_{MAM}$	1.37	6.02 ^{NS}	0.76 ^{NS}	1.09	12.34**	0.73 ^{NS}
CLOUD$_{JJA}$	1.10	6.14 ^{NS}	0.64 ^{NS}	1.00	9.05**	0.69 ^{NS}
CLOUD$_{ANNUAL}$	1.00	6.83*	0.88 ^{NS}	1.00	12.58**	0.75 ^{NS}
RWL$_{ANNUAL}$	1.72	6.87*	0.64 ^{NS}	1.94	26.10***	0.86 ^{NS}
RWL$_{MAM}$	1.00	10.19**	0.85 ^{NS}	3.14	15.09***	0.73 ^{NS}
RWL$_{JJA}$	1.40	5.00 ^{NS}	0.88 ^{NS}	1.00	10.10**	0.77 ^{NS}
FAI	3.08	6.14 ^{NS}	0.85 ^{NS}	2.58	5.16 ^{NS}	0.85 ^{NS}
PE	1.77	7.33**	0.66 ^{NS}	1.00	8.08*	0.29 ^{NS}
AI	3.42	9.55**	0.68 ^{NS}	1.66	15.00***	0.60 ^{NS}
PDSI	2.92	16.21**	0.88 ^{NS}	1.00	40.95***	0.75 ^{NS}
SPI$_6$ Aug	1.00	5.08 ^{NS}	0.92 ^{NS}	1.00	20.23***	0.57 ^{NS}
SPI$_{12}$ Aug	1.57	5.83 ^{NS}	0.84 ^{NS}	1.37	5.19 ^{NS}	0.63 ^{NS}
SPEI$_6$ Aug	1.73	12.24**	0.79 ^{NS}	1.13	5.02 ^{NS}	0.66 ^{NS}
SPEI$_{12}$ Aug	3.19	8.72**	0.92 ^{NS}	5.08	10.68**	0.73 ^{NS}
	Adj. R^2 = 0.283		K = 9	Adj. R^2 = 0.299		K = 9
	N = 300			N = 300		
	GCV = 0.061517			GCV = 0.000759		
Turkey oak (*Quercus cerris* L.)						
	TRWi			**det. δ^{13}C**		
Variable	**EDF**	**F (p)**	**k-index (p)**	**EDF**	**F (p)**	**k-index (p)**
TEMP$_{MAM}$	1.33	7.46*	0.97 ^{NS}	2.52	15.50***	0.83 ^{NS}
TEMP$_{JJA}$	1.17	5.01 ^{NS}	0.82 ^{NS}	3.66	8.04*	1.00 ^{NS}
TEMP$_{ANNUAL}$	1.39	5.02 ^{NS}	0.95 ^{NS}	1.55	5.02 ^{NS}	0.99 ^{NS}
PRCP$_{ANNUAL}$	2.69	7.20*	0.76 ^{NS}	2.59	23.89***	0.98 ^{NS}
PRCP$_{MAM}$	1.00	9.83**	0.91 ^{NS}	1.00	9.38**	0.99 ^{NS}
PRCP$_{JJA}$	2.08	5.03 ^{NS}	0.99 ^{NS}	1.37	5.75 ^{NS}	0.99 ^{NS}
CLOUD$_{MAM}$	1.00	5.71 ^{NS}	0.97 ^{NS}	3.55	9.55**	0.97 ^{NS}
CLOUD$_{JJA}$	1.34	22.96***	0.99 ^{NS}	1.00	32.60***	0.99 ^{NS}
CLOUD$_{ANNUAL}$	3.48	14.24***	0.93 ^{NS}	2.41	10.59**	0.99 ^{NS}
RWL$_{ANNUAL}$	1.83	6.93 ^{NS}	0.95 ^{NS}	1.27	7.08*	0.97 ^{NS}
RWL$_{MAM}$	1.00	14.16**	0.89 ^{NS}	1.00	12.44**	0.98 ^{NS}
RWL$_{JJA}$	1.00	11.73**	0.95 ^{NS}	2.97	14.95**	0.99 ^{NS}
FAI	1.92	5.16 ^{NS}	0.86 ^{NS}	1.00	5.10 ^{NS}	0.98 ^{NS}
PE	1.00	5.29 ^{NS}	0.98 ^{NS}	6.45	14.56***	0.99 ^{NS}
AI	1.88	15.84***	0.99 ^{NS}	2.05	19.04***	0.67 ^{NS}
PDSI	1.00	65.62***	0.94 ^{NS}	1.86	17.16***	0.95 ^{NS}
SPI$_6$ Aug	1.64	7.47*	0.94 ^{NS}	3.35	8.61*	0.97 ^{NS}
SPI$_{12}$ Aug	2.70	13.55***	0.90 ^{NS}	1.07	7.52*	0.98 ^{NS}
SPEI$_6$ Aug	3.89	9.62**	0.92 ^{NS}	1.00	5.06 ^{NS}	0.96 ^{NS}
SPEI$_{12}$ Aug	1.00	6.67*	0.94 ^{NS}	1.00	7.03*	0.97 ^{NS}
Adj. R^2 = 0.541			K = 9	Adj. R^2 = 0.646		K = 9
N = 300				N = 300		
GCV = 0.000793				GCV = 0.052782		

Note: GAMM – Generalized additive mixed model; EDF – Estimated degree of freedom; F – Fisher test; *p* – statistical significance. Signif. code: (^{NS}) – non-significant; (*) < 0.1, (**) < 0.01; (***) < 0.001. Time span = 1961–2010.

especially in the last decade of the analysed time span (2001–2010).

Drought was visually interpreted using the combined drought index (X_{12} Dec and X_6 Aug) in Fig. 3. Both X_{12} Dec and X_6 Aug were chosen as they represent the average of the two drought indices (SPI and SPEI), which were (each separately) used in the analyses of TRW and $\delta^{13}C$ sensitivity to drought, via the GAMM. In the covered time span (1960–2010), extremely wet (positive values) and extremely dry (negative values) years were analysed on a year-to-year basis. Four extremely dry years (X_{12} and $X_6 < -2$) were identified: 2003 (X_6 −2.9), 2000 (X_6 −2.02), 1961 (X_6 −2.14) and 1960 (X_6 −2.25). Four moderately dry years (X_{12} and X_6 −1 to −2) were identified (1971, 1990, 1992 and 2002) regardless of the type of drought index. Based on the X_{12}Dec variations we also identified several dry and wet periods. The dry periods were 1960–1963, 1983–1990 and 2007–2009 and the wet periods were 1995–1999 and 2004–2006 (Fig. 3).

3.2. QURO and QUCE TRW, $\delta^{13}C$ and iWUE variations

The stable carbon isotope ratio and radial increment sensitivity to environmental conditions varied over time and among the studied oak species (see Fig. 4). In the analysed time span, QURO and QUCE had similar TRW characteristics (QURO 1.72 mm year^{-1}; QUCE 1.42 mm year^{-1}; Fig. 4c). In the same 50-year period, on the other hand, the QURO and QUCE $\delta^{13}C$ values responded differently to climate drivers. In 48 out of the 50 analysed years (96 % of years) from 1960 to 2010, QUCE (-25.41) had a more negative $\delta^{13}C$ value than QURO (-24.76); see chronologies in Fig. 4a and their range in Fig. 5. The aforementioned associations between QURO and QUCE $\delta^{13}C$ chronologies exhibited a high level of synchronicity, as opposed to TRW, based on Kendall's Tau correlation coefficient ($\delta^{13}C$ τ = 0.67). High similarity was also observed between iWUE chronologies (τ = 0.74). Likewise, larger deviations in $\delta^{13}C$ compared to TRW between the analysed oak species were noted in response to different drought indices.

Calculated values for the iWUE parameter over time show an increasing trend as we approach the present (Fig. 4b). This relates to tree adaptation to the changing environment. The observed increasing trend is caused by an increasing amount of CO_2 in the atmosphere and decreasing v^{13}C content in the atmosphere due to the use of fossil fuels (both parameters are inputs in the iWUE equation; see Eq. (2)). Likewise, the QURO-QUCE differences in iWUE deviate in the same two years (1967 and 1971) as $\delta^{13}C$, which is expected as iWUE is modelled based on wood cellulose and atmospheric $\delta^{13}C$ values (Fig. 5).

We found differences between the average stable isotope ratio in the latewood of QUCE and QURO tree rings. Average $\delta^{13}C$ in the period 1961–2010 was −24.77 ‰ for QURO and −25.43 ‰ for QUCE. Both studied species responded similarly; however, QURO $\delta^{13}C$ is always less negative in both dry and wet conditions than QUCE. The most negative values of $\delta^{13}C$ in the whole QUCE chronology were noted in 2004 and 2005 (-27.05 ‰ and −26.66 ‰) in the wettest period of the entire analysed time period (values of X_6 Aug 1.36 and 1.95). The third largest negative $\delta^{13}C$ peak was noted in 1997 (QUCE −26.59 ‰), which corresponds well with the wet period 1995–1999. $\delta^{13}C$ values in wet years in QURO were not as negative as those in the latewood of QUCE tree rings.

Stable isotope values of QUCE and QURO in extremely wet years were rather different in terms of absolute values. QUCE seems to be more responsive to a wetter climate than QURO; in the 2003–2005 period, QUCE had more negative $\delta^{13}C$ values than QURO. Apart from a few extremely dry years (1967, 1971, 1979 and 1989/90), when $\delta^{13}C$ values were least negative and almost identical for both species, QUCE seems to respond more sensitively to wet years in comparison to QURO (Fig. 4a).

TRW chronologies of QURO and QUCE were analysed as raw measurements (Fig. 4c). Larger TRW peaks were noted in QURO. In wetter years in particular, QURO grew much better than QUCE. In the optimal wet year of 1978 (X_{12} Dec 0.15), TRW was 2.73 mm and in 1975 (X_{12}

Dec 0.75) TRW was 2.54 mm. In the extreme wet year of 2001 (X_{12} Dec 2.26), TRW was 2.65 mm and in the wet year of 1970 (X_{12} Dec 1.52), TRW was 2.52 mm. Additionally, Fig. 4c shows a delayed response in TRW to changing growing conditions. The period 2003–2005 is followed by a dry period and both species responded with a delay; however, QUCE reacted more quickly, with a more intense growth reduction than that of QURO.

We noted moderate to high synchrony between the TRW chronologies of QURO and QUCE (τ = 0.43) and higher synchrony between $\delta^{13}C$ chronologies (τ = 0.67) and iWUE chronologies (τ = 0.74) (Fig. 5). The differences between the TRW chronologies of QURO and QUCE are presented as QUCE TRW chronology deviations from the QURO TRW chronology. The QURO and QUCE TRW chronologies exhibit similar responses, but slightly decreasing QUCE TRW troughs were noted in 1968 (caused by drought in 1966–1968), ~ the 1990 s and in the mid-2000 s. After the 1990 s and two significant QURO mortality events in the 1980 s, the TRW of QURO decreased up to the 2000 s and aligned with the downward trend of the TRW chronology of QUCE. The observed stronger decrease in the TRW of QUCE after the first major drought event (1966–1968) in the analysed chronology is repeated after the strongest drought event in 2006, when QURO exhibits a faster recovery than that of QUCE. The smallest differences between QUCE and QURO were observed in stable isotopes. Deviations did not show a trend and remained constant throughout the studied period. Deviations between species with regard to iWUE were moderate; however, a weak trend can be observed as we approach the present time. Thus, differences in iWUE between QUCE and QURO are increasing, and one species is benefiting from the increasing CO_2 concentrations in the atmosphere and the other is not (Fig. 5).

### 3.3. QURO and QUCE $\delta^{13}C$ and TRW association with surrounding factors

Pedunculate and Turkey oaks strongly respond to stand conditions. The response of TRW, TRWi and $\delta^{13}C$ to surrounding factors is visually presented in Fig. 4. According to the TRW and $\delta^{13}C$ measurements (Fig. 4a and 4c), in most cases both oaks responded similarly to environmental stressors. Likewise, the GAMM spline indicates that their response to stressors is nonlinear (Table 1). The precipitation parameters (PRCP$_{MAM}$, PRCP$_{JJA}$ and PRCP$_{ANNUAL}$) are mostly linear (see estimated degree of freedom (EDF) values in Table 1). According to the precipitation parameter (PRCP$_{MAM}$, PRCP$_{JJA}$ and PRCP$_{ANNUAL}$) values, moderate stand wetness boosts TRW, which is suppressed under extremely dry and wet conditions (Fig. 4a). As intensive tree growth occurs during the warmer time of the year (late spring and summer months), cloudiness (as measured by CLOUD$_{MAM}$, CLOUD$_{JJA}$ and CLOUD$_{ANNUAL}$) mitigates the effects of excessive warming and exerts a positive effect on TRW. Our findings further revealed that TRW and $\delta^{13}C$ were also affected by river water level (RWL$_{MAM}$, RWL$_{JJA}$ and RWL$_{ANNUAL}$), whereby higher RWL values were positively correlated with TRW.

The six drought indices included in this study suggest that both $\delta^{13}C$ and TRW are sensitive to drought, but that the degree of sensitivity is species-specific. As expected, the FAI, PE and AI indices show that the greatest TRW occurs when the analysed oaks grew in optimal conditions. On the other hand, TRW was found to be less sensitive to 6- and 12-month SPIs and SPEIs than $\delta^{13}C$, the response of which is much stronger to these factors.

Meteorological parameters, drought indices and river water level were included in the GAMM model to interpret their impact on det. $\delta^{13}C$ and TRWi. As shown in Table 1, 20 variables were included in the TRWi and det. $\delta^{13}C$ GAMMs. Our findings revealed that a better fit was achieved for det. $\delta^{13}C$ and QUCE, as confirmed by the adjusted coefficient of determination (Adj. R^2) of 0.646 for det. $\delta^{13}C$. Likewise, the higher Adj. R^2 obtained for the QURO $\delta^{13}C$ GAMM (0.299) was compared with the QURO TRWi GAMM (0.283). The four analysed GAMM models failed to reveal unique QURO and QUCE TRWi and $\delta^{13}C$ patterns, but some
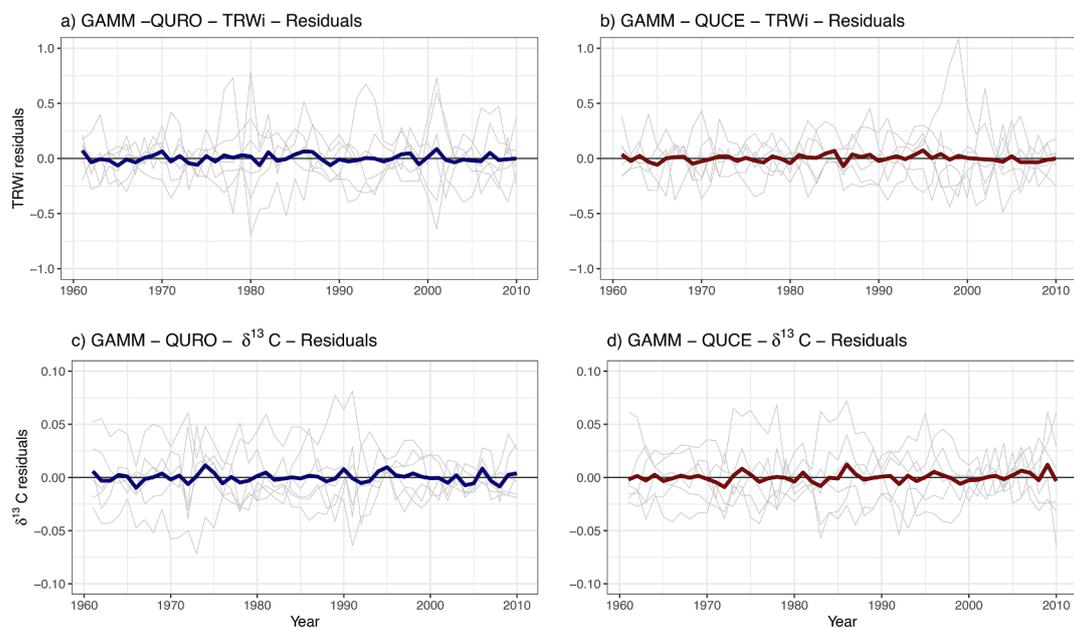
Fig. 6. GAMM residuals for pedunculate (blue line) and Turkey oak (red line) detrended radial growth (TRWi) and detrended stable carbon isotope ratio (det. δ^{13}C) for the 1961–2010 time span. (For interpretation of the references to colour in this figure legend, the reader is referred to the web version of this article.)
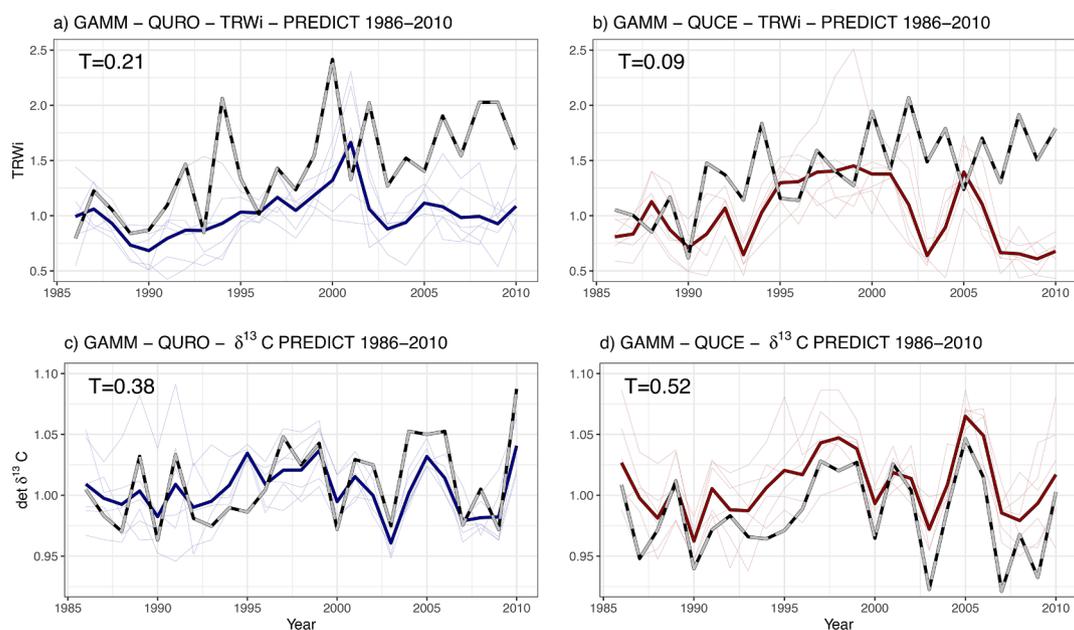
Fig. 7. GAMM model validation to detrended radial growth and stable carbon isotope chronology, separated into QURO (**a, b**) and QUCE (**c, d**) data. The solid line represents measured and the dashed line simulated data for 1986–2010 based on the GAMM (Eq. (4)) and data from 1961 to 1985.

trends were nevertheless noted. For example, annual temperature (TEMP$_{ANNUAL}$) and FAI were not a statistically significant (for $p < 0.05$) variable in any of the four GAMM models. Temperature and precipitation in summer months (JJA) had a non-significant influence on TRWi. On the other hand, det. δ^{13}C had an equal response to summer and spring months for QURO. As can be seen from the GAMM residuals shown in Fig. 6, significant deviations cannot be detected in the data across the analysed 50-year time span.

Radial growth and det. δ^{13}C prediction potential based on the 20 different variables were tested using the GAMM, whereby 50-year-long chronologies were split into two subsets for calibration and validation. The GAMM predictions were calibrated using the first 25 years

(1961–1985), while the second subset (1986–2010) was used for the model validation (see Fig. 7). Measured and predicted chronologies were compared using Kendall Tau statistics, which indicated that det. δ^{13}C was a more reliable predictor for climate and environmental factors than TRWi chronologies. Both oak species exhibited high similarity between measured and predicted det. δ^{13}C and low similarity for TRWi GAMMs. Apparent weaknesses of the constructed GAMMs are noted in extreme years. Trees in extreme years (e.g. 2000 and 2010) showed a less pronounced response than model predictions; therefore, longer trends are appropriate for a deeper interpretation than single years.

4. Discussion

4.1. Are differences in TRW, $\delta^{13}C$ and iWUE between QURO and QUCE caused by species-specific responses?

The growth response of trees to climate conditions is controlled by several surrounding site factors and their interactions (Pretzsch, 2009; Roman et al., 2015). Additionally, specific cross-talk through the plant and species-specific response play a role in radial increment and stomata regulation and sensitivity to stress conditions (which define the $^{12}C/^{13}C$ ratio), depending on fractionation processes during the photosynthetic uptake of CO_2 via the stomata (Farquhar et al., 1989; Lakatos et al., 2007).

The QURO and QUCE $\delta^{13}C$ chronologies have identical patterns, but QUCE exhibits more negative $v^{13}C$ across the entire time span, which indicates different adaptive potential to lack of water and drought periods than that of QURO. Tree productivity (radial growth) and its isotopic responses ($\delta^{13}C$) are not necessarily linked. Their relations should be limited by the spatial arrangement of trees in the forest ecosystem. Shestakova et al. (2019) observed that $\delta^{13}C$ relations with TRW are weaker in colder climate zones (boreal and temperate climate zones) in contrast to warmer, e.g. Mediterranean, climate zones on the European scale. Additionally, a prolonged effect (up to three years) of the TRW response (Stojanović et al., 2018) and faster $\delta^{13}C$ response to climate conditions (Zheng et al., 2019) contribute to the absence of a relationship, which was confirmed in our study.

Different climate sensitivities were observed between oak species and radial growth and stable carbon isotope chronologies. Generally, QURO, as the slightly less drought-resistant species, was recognized as more climate and drought sensitive, which is in line with studies by Levanič et al. (2011), Cailleret et al. (2018) and Sun et al. (2018), who agreed that trees with lower performances and/or in stress conditions (e. g. declining vs healthy trees) are more climate-sensitive. On the other hand, drought and stress conditions did not affect the inter-species variability of wood production, in contrast to differences in $\delta^{13}C$ content.

The calculated iWUE interpreted stomatal water loss as a function of the amount of CO_2 assimilated (Farquhar et al., 1982; Nock et al., 2011). Despite the generally increasing trend in iWUE, in years with more favourable climate conditions, we also observed decreasing iWUE, which is an indication of the adaptive potential of both studied species. A similar decrease in iWUE in favourable conditions has been observed in many tree species, such as ponderosa pine (McDowell et al., 2010), bur oak (Voelker et al., 2014) and Scots pine (Timofeeva et al., 2017), throughout the 20th century.

4.2. Are drought indices reliable indicators of variation in radial growth and $\delta^{13}C$?

Temperature, precipitation and six different meteorological drought indices were included in the radial growth and stable carbon isotope ratio drought-sensitivity analyses. As expected, stronger interactions with different combinations of spring and early summer climate parameters and drought indices (see Table 1) of the year of tree-ring formation were obtained for $\delta^{13}C$ and drought indices because stomatal closure (which causes entry of the heavier stable ^{13}C isotope into the Calvin cycle, also known as fractionation due to carboxylation) can change quickly, in contrast to the slower radial growth response (Martin-StPaul et al., 2017; Huang et al., 2018; Stojanović et al., 2018; Zheng et al., 2019). The second reason for the stronger interaction of stable carbon isotope with drought indices may be related to the analysis of latewood only for $\delta^{13}C$ in this study, although the same phenomena were observed in several previously published studies where whole tree-rings were used (Zheng et al., 2019). In addition, Hafner et al. (2015) noted that $\delta^{13}C$ in the latewood of pedunculate oak (from the same geomorphological entity) strongly correlates with summer (June-August) climate and drought indices of the year of tree-ring formation.

Strong correlations between radial growth, $\delta^{13}C$ and meteorological drought indices were observed in our study as well as in many previously published dendroecological papers. For example, Timofeeva et al. (2017) found that the stable carbon isotope ratio and TRW in Scots pine were sensitive to variations in the SPEI. Stojanović et al. (2018) analysed the drought sensitivity of QURO and QUCE and obtained a strong correlation between TRW and the SPEI (time scale of 3 to 36 months), while Billings et al. (2016) observed a strong correlation between the PDSI and C and O stable isotope ratios in red oak (*Quercus rubra* L.).

Zheng et al. (2019) tested radial growth and stable carbon isotope ratio sensitivity against several meteorological parameters, including different meteorological drought indices. Similar to our study, Zheng et al. (2019) revealed a stronger correlation between radial growth, stable carbon isotope ratio and calculated drought indices ($SPEI_6$ and PDSI) with basic meteorological measurements (temperature, precipitation, humidity, cloudiness, etc.). Out of the eight tested basic meteorological measurements, only two, relative humidity and vapour pressure deficit, had a significant effect on tree-ring widths or stable carbon isotope ratios.

5. Concluding remarks

Species-specific variations in radial growth and stable carbon isotope ratio between Turkey oak and pedunculate oak were analysed. The results presented in this study suggest that Turkey oak is more sensitive to environmental factors in both $\delta^{13}C$ and radial growth. Compared to pedunculate oak, Turkey oak exhibited lower radial growth and more negative $\delta^{13}C$ throughout the analysed period. According to the GAMM outputs, the more drought-tolerant Turkey oak showed better adaptation to stand environmental and climatic factors compared to pedunculate oak.

We observed species-specific responses to site conditions (interpreted via river water level, meteorological factors and drought indices) and found that the analysed tree-ring properties (radial growth and $\delta^{13}C$) were differentially sensitive to stand environmental and climatic factors.

To summarize, we gained new insights into the relationships between stable carbon isotope records, radial growth and climate, and drought and environmental conditions in two oak species. For forest practitioners, a deeper understanding of species-specific response to changing environmental conditions is necessary to mitigate the negative effects of climate change on oak forests. This is particularly important for the coming period, when climatic change is expected to intensify and drought-sensitive forests (such as lowland oak forests) will be even more vulnerable than they are now.

CRediT authorship contribution statement

Saša Kostić: Writing – original draft, Writing – review & editing, Conceptualization, Visualization, Methodology, Formal analysis, Validation, Software. **Tom Levanič:** Writing – original draft, Writing – review & editing, Conceptualization, Visualization, Methodology, Formal analysis, Validation, Funding acquisition, Project administration, Resources, Supervision, Data curation, Software. **Saša Orlović:** Funding acquisition, Project administration, Resources, Supervision. **Bratislav Matović:** Methodology, Investigation, Writing – review & editing. **Dejan B. Stojanović:** Writing – original draft, Writing – review & editing, Conceptualization, Visualization, Methodology, Formal

analysis, Validation, Funding acquisition, Project administration, Resources, Supervision, Data curation, Software.

Declaration of Competing Interest

The authors declare that they have no known competing financial interests or personal relationships that could have appeared to influence the work reported in this paper.

Data availability

Data will be made available on request.

Acknowledgement

We are grateful to the Vojvodinašume enterprise for their assistance with tree sampling. The authors thank anonymous reviewers for their thoughtful and constructive suggestions.

Appendix A

Table A1

Table A1
Abbreviations, descriptions and sources of the GAMM variables.

No.	Abbreviation	Variable	Description	Source
1	PRCP$_{ANNUAL}$	Annual sum of precipitation	Units: mm m^{-2}, frequency: daily measurements.	E-OBS, 23.1e version (Copernicus: European Union's Earth observation programme)
2	PRCP$_{MAM}$	March-May sum of precipitation		
3	PRCP$_{JJA}$	June-August sum of precipitation		
4	PRCP$_{Y2}$	Two-year sum of precipitation		
5	TEMP$_{ANNUAL}$	Annual temperature	Units: °C, frequency: daily measurements.	
6	TEMP$_{MAM}$	March-May average temperature		
7	TEMP$_{JJA}$	June-August average temperature		
8	TEMP$_{Y2}$	Two-year average temperature		
9	RWL$_{ANNUAL}$	Annual river water level	River water level (cm), frequency: daily observations.	Hydrometeorological Services of Republic of Serbia
10	RWL$_{MAM}$	March-May river water level		
11	RWL$_{JJA}$	June-August river water level		
12	SPEI	Standardized evaporation index	Calculated from daily data from E-OBS data base.	E-OBS, 23.1e version (Copernicus: European Union's Earth observation programme)
13	SPI	Standard precipitation index		
14	FAI	Forestry aridity index		
15	PE	Potential evaporation		
16	AI	Aridity index		
17	PDSI	Palmer drought severity index		

References

Adams, H.D., Zeppel, M.J.B., Anderegg, W.R.L., et al., 2017. A multi-species synthesis of physiological mechanisms in drought-induced tree mortality. Nat. Ecol. Evol. 1 (9), 1285–1291.

Alexandrov, A.H., Iliev, I., 2019. Forests in South-eastern Europe. Poplar 203, 79–85.

Allen, C.D., Macalady, A.K., Chenchouni, H., et al., 2010. A global overview of drought and heat-induced tree mortality reveals emerging climate change risks for forests. Forest Ecol. Manag. 259 (4), 660–684.

Annighöfer, P., Beckschäfer, P., Vor, T., Ammer, C., 2015. Regeneration patterns of European oak species (*Quercus petraea* (Matt.) Liebl., *Quercus robur* L.) in dependence of environment and neighborhood. PLoS ONE 10 (8), e0134935.

Arvai, M., Morgos, A., Kern, Z., 2018. Growth-climate relations and the enhancement of drought signals in Pedunculate oak (*Quercus robur* L.) tree-ring chronology in Eastern Hungary. iForest, 11(2), 267.

Assal, T.J., Anderson, P.J., Sibold, J., 2016. Spatial and temporal trends of drought effects in a heterogeneous semi-arid forest ecosystem. Forest Ecol. Manage. 365, 137–151.

Billings, S.A., Boone, A.S., Stephen, F.M., 2016. Tree-ring δ^{13}C and δ^{18}O, leaf δ^{13}C and wood and leaf N status demonstrate tree growth strategies and predict susceptibility to disturbance. Tree Physiol. 36 (5), 576–588.

Bugmann, H., Pfister, C., 2000. Impacts of interannual climate variability on past and future forest composition. Reg. Environ. Change. 1, 112–125.

Bunn, A.G., 2008. A dendrochronology program library in R (dplR). Dendrochronologia 26 (2), 115–124.

Büntgen, U., Kolář, T., Rybníček, M., et al., 2020. No age trends in oak stable isotopes. Paleoceanogr. Paleocl. 35(4), e2019PA003831.

Büntgen, U., Tegel, W., Nicolussi, K., et al., 2011. 2500 years of European climate variability and human susceptibility. Science 331 (6017), 578–582.

Cailleret, M., Dakos, V., Jansen, S., et al., 2018. Early-warning signals of individual tree mortality based on annual radial growth. Front. Plant Sci. 9, 1964.

Cornes, R.C., van der Schrier, G., van den Besselaar, E.J., Jones, P.D., 2018. An ensemble version of the E-OBS temperature and precipitation data sets. J. Geophys. Res. Atmos. 123 (17), 9391–9409.

Csank, A.Z., Miller, A.E., Sherriff, R.L., Berg, E.E., Welker, J.M., 2016. Tree-ring isotopes reveal drought sensitivity in trees killed by spruce beetle outbreaks in south-central Alaska. Ecol. Appl. 26 (7), 2001–2020.

De Martonne, E., 1925. Traité de Géographie Physique. Colin, Paris, France, p. 11.

Farquhar, G.D., Ehleringer, J.R., Hubick, K.T., 1989. Carbon isotope discrimination and photosynthesis. Annu. Rev. Plant Physiol. Plant Mol. Biol. 40 (1), 503–537.

Farquhar, G., O'Leary, M., Berry, J., 1982. On the relationship between carbon isotope discrimination and the intercellular carbon dioxide concentration in leaves. Funct. Plant Biol. 9, 121–137.

Fritts, H.C., 2001. Tree rings and climate. Blackburn Press, Caldwell.

Führer, E., Horvath, L., Jagodics, A., Machon, A., Szabados, I., 2011. Application of new aridity index in Hungarian forestry practice. Quarterly J. Hungarian Meteorol. Ser. 115, 205–216.

Gholami, V., Sahour, H., Torkaman, J., 2021. Monthly river flow modeling using earlywood vessel feature changes, and tree-rings. Ecol. Indic. 125, 107590.

Haavik, L.J., Billings, S.A., Guldin, J.M., Stephen, F.M., 2015. Emergent insects, pathogens and drought shape changing patterns in oak decline in North America and Europe. For. Ecol. Manage. 354, 190–205.

Hafner, P., Robertson, I., McCarroll, D., Loader, N., Gagen, M., Bale, R., Jungner, H., Sonninen, E., Hilasvuori, E., Levanič, T., 2011. Climate signals in the ring widths and stable carbon, hydrogen and oxygen isotopic composition of *Larix decidua* growing at the forest limit in the southeastern European Alps. Trees Struct. Funct. 25, 1141–1154.

Hafner, P., Gričar, J., Skudnik, M., Levanič, T., 2015. Variations in environmental signals in tree-ring indices in trees with different growth potential. PloS one 10 (11), e0143918.

Hamed, K.H., 2011. The distribution of Kendall's tau for testing the significance of cross-correlation in persistent data. Hydrolog. Sci. J. 56 (5), 841–853.

Hoffmann, N., Schall, P., Ammer, C., Leder, B., Vor, T., 2018. Drought sensitivity and stem growth variation of nine alien and native tree species on a productive forest site in Germany. Agric. For. Meteorol. 256, 431–444.

Huang, M., Wang, X., Keenan, T.F., Piao, S., 2018. Drought timing influences the legacy of tree growth recovery. Glob. Change Biol. 24 (8), 3546–3559.

IPCC, I. P. O. C. C. (2019). Special report on global warming of 1.5 C (SR15).

Keenan, R.J., 2015. Climate change impacts and adaptation in forest management: a review. Ann. For. Sci. 72, 145–167.

Kostić, S., Wagner, W., Orlović, S., et al., 2021b. Different tree-ring width sensitivities to satellite-based soil moisture from dry, moderate and wet Pedunculate oak (*Quercus robur* L.) stands across a southeastern distribution margin. Sci. Total Environ. 800, 149536.

Kostić, S., Kesić, L., Matović, B., Orlović, S., Stojnić, S., Stojanović, D.B., 2021a. Soil properties are significant modifiers of Pedunculate oak (*Quercus robur* L.) radial increment variations and their sensitivity to drought. Dendrochronologia 67, 125838.

Kostić, S., Orlović, S., Karaklić, V., Kesić, L., Zorić, M., Stojanović, D.B., 2021c. Allometry and post-drought growth resilience of pedunculate oak (*Quercus robur* L.) varieties. Forests 12 (7), 930.

Kottek, M., Grieser, J., Beck, C., Rudolf, B., Rubel, F., 2006. World map of the Köppen-Geiger climate classification updated. Meteorol. Z. 15, 259–263.

Kramer, H. *Waldwachstumslehre*; Verlag Paul Parey: Hamburg, Berlin, 1988; pp. 374.

Lakatos, M., Hartard, B., Máguas, C., 2007. The stable isotopes δ13C and δ18O of lichens can be used as tracers of micro environmental carbon and water sources. Terrest Ecol 1, 77–92.

Landi, M., Cotrozzi, L., Pellegrini, E., et al., 2019. When "thirsty" means "less able to activate the signalling wave trigged by a pulse of ozone": A case of study in two Mediterranean deciduous oak species with different drought sensitivity. Sci. Total Environ. 657, 379–390.

Levanič, T., 2007. ATRICS–A new system for image acquisition in dendrochronology. Tree-Ring Res. 63 (2), 117–122.

Levanič, T., Čater, M., McDowell, N.G., 2011. Associations between growth, wood anatomy, carbon isotope discrimination and mortality in a *Quercus robur* forest. Tree Physiol. 31 (3), 298–308.

Loader, N.J., Robertson, I., Barker, A.C., et al., 1997. An improved technique for the batch processing of small wholewood samples to α-cellulose. Chem. Geol. 136, 313–317.

Loader, N.J., Santillo, P.M., Woodman-Ralph, J.P., et al., 2008. Multiple stable isotopes from oak trees in southwestern Scotland and the potential for stable isotope dendroclimatology in maritime climatic regions. Chem. Geol. 252 (1–2), 62–71.

Loader, N.J., McCarroll, D., Miles, D., Young, G.H.F., Davies, D., Ramsey, C.B., 2019. Tree ring dating using oxygen isotopes: a master chronology for central England. J. Quat. Sci. 34, 475–490.

Losseau, J., Jonard, M., Vincke, C., 2020. Pedunculate oak decline in southern Belgium: a long-term process highlighting the complex interplay among drought, winter frost, biotic attacks, and masting. Can. J. For. Res. 50 (4), 380–389.

Martin-StPaul, N., Delzon, S., Cochard, H., Maherali, H., 2017. Plant resistance to drought depends on timely stomatal closure. Ecol. Lett. 20 (11), 1437–1447.

McCarroll, D., Loader, N.J., 2004. Stable isotopes in tree rings. Quaternary Sci. Rev. 23 (7–8), 771–801.

McDowell, N.G., Allen, C.D., Marshall, L., 2010. Growth, carbon-isotope discrimination, and drought-associated mortality across a *Pinus ponderosa* elevational transect. Glob. Chang Biol. 16, 399–415.

McDowell, N.G., Allen, C.D., Anderson-Teixeira, K., et al., 2020. Pervasive shifts in forest dynamics in a changing world. Science 368 (6494), eaaz9463.

McDowell, N., Pockman, W.T., Allen, C.D., Breshears, D.D., Cobb, N., Kolb, T., Plaut, J., Sperry, J., West, A., Williams, D.G., Yepez, E.A., 2008. Mechanisms of plant survival and mortality during drought: why do some plants survive while others succumb to drought? New Phytol. 178 (4), 719–739.

McKee, T.B., Doesken, N.J., Kleist, J., 1993. The relationship of drought frequency and duration to time scales. Proceedings of the Eighth Conference on Applied Climatology, Boston, MA: American Meteorological Society.

Nechita, C., Eggertsson, O., Badea, O.N., Popa, I., 2018. A 781-year oak tree-ring chronology for the Middle Ages archaeological dating in Maramureş (Eastern Europe). Dendrochronologia 52, 105–112.

Netsvetov, M., Prokopuk, Y., Puchałka, R., et al., 2019. River regulation causes rapid changes in relationships between floodplain oak growth and environmental variables. Front. Plant. Sci. 10, 96.

Neuwirth, B., Rabbel, I., Bendix, J., Bogena, H.R., Thies, B., 2021. The European Heat Wave 2018: The dendroecological response of oak and spruce in Western Germany. Forests 12 (3), 283.

Nock, C.a., Baker, P.j., Wanek, W., Leis, A., Grabner, M., Bunyavejchewin, S., Hietz, P., 2011. Long-term increases in intrinsic water-use efficiency do not lead to increased stem growth in a tropical monsoon forest in western Thailand. Glob. Change Biol. 17 (2), 1049–1063.

Palmer, W.C., 1965. Meteorological drought. research paper No. 45. US Weather Bureau, Washington, DC, USA.

Pretzsch, H., 2009. Forest dynamics, growth and yield. Springer, Berlin, Heidelberg.

R Core Team, 2013. R: A language and environment for statistical computing. Austria, Vienna.

Roman, D.T., Novick, K.A., Brzostek, E.R., et al., 2015. The role of isohydric and anisohydric species in determining ecosystem-scale response to severe drought. Oecologia 179 (3), 641–654.

Ruosteenoja, K., Markkanen, T., Venäläinen, A., Räisänen, P., Peltola, H., 2018. Seasonal soil moisture and drought occurrence in Europe in CMIP5 projections for the 21st century. Clim. Dyn. 50 (3–4), 1177–1192.

Saurer, M., Siegwolf, R.T.W., 2007. Human impacts on tree-ring growth reconstructed from stable isotopes. In: Dawson, T.E., Siegwolf, R.T.W. (Eds.), Stable Isotopes as Indicators of Ecological Change. Elsevier, pp. 49–62.

Schnabel, F., Purrucker, S., Schmitt, L., Engelmann, R.A., Kahl, A., Richter, R., Seele-Dilbat, C., Skiadaresis, G., Wirth, C., 2022. Cumulative growth and stress responses to the 2018–2019 drought in a European floodplain forest. Glob. Chang. Biol. 28 (5), 1870–1883.

Shestakova, T.A., Voltas, J., Saurer, M., et al., 2019. Spatio-temporal patterns of tree growth as related to carbon isotope fractionation in European forests under changing climate. Global Ecol. Biogeogr. 28 (9), 1295–1309.

Skiadaresis, G., Schwarz, J.A., Bauhus, J., 2019. Groundwater extraction in floodplain forests reduces radial growth and increases summer drought sensitivity of Pedunculate oak trees (*Quercus robur* L.). Front. For. Glob. Change 2, 5.

Spinoni, J., Naumann, G., Vogt, J.V., Barbosa, P., 2015. The biggest drought events in Europe from 1950 to 2012. J. Hydrol. Reg. Stud. 3, 509–524.

Stojanović, D.B., Levanič, T., Matović, B., Orlović, S., 2015. Growth decrease and mortality of oak floodplain forests as a response to change of water regime and climate. Eur. J. For. Res. 134 (3), 555–567.

Stojanović, D.B., Levanič, T., Matović, B., Stjepanović, S., Orlović, S., 2018. Growth response of different tree species (oaks, beech and pine) from SE Europe to precipitation over time. Dendrobiology 79, 97–110.

Sun, S., He, C., Qiu, L., Li, C., Zhang, J.S., Meng, P., 2018. Stable isotope analysis reveals prolonged drought stress in poplar plantation mortality of the Three-North Shelter Forest in Northern China. Agric. For. Meteorol. 252, 39–48.

Thornthwaite, C.W., 1948. An approach toward a rational classification of climate. Geogr. Rev. 38 (1), 55–94.

Timofeeva, G., Treydte, K., Bugmann, H., Rigling, A., Schaub, M., Siegwolf, R., Saurer, M., 2017. Long-term effects of drought on tree-ring growth and carbon isotope variability in Scots pine in a dry environment. Tree Physiol. 37 (8), 1028–1041.

Vicente-Serrano, S.M., Begueria, S., Lopez-Moreno, J.I., 2010. A multi-scalar drought index sensitive to global warming: the Standardized Precipitation Evapotranspiration Index. J. Clim. 23, 1696–1718.

Voelker, S.L., Meinzer, F.C., Lachenbruch, B., Brooks, J.R., Guyette, R.P., 2014. Drivers of radial growth and carbon isotope discrimination of bur oak (*Quercus macrocarpa* Michx.) across continental gradients in precipitation, vapour pressure deficit and irradiance. Plant Cell Environ. 37, 766–779.

Wickham, H., 2016. ggplot2: Elegant graphics for data analysis. Springer-Verlag, New York. (Available at: https://ggplot2.tidyverse.org).

Wood, S.N., 2017. Generalized additive models: an introduction with R. CRC Press.

Wood, S., Wood, M.S., 2015. Package 'mgcv'. R package version, 1, 29.

Yee, T.W., 2010. The VGAM package for categorical data analysis. J. Statist. Softw. 32 (10), 1–34.

Zheng, W., Gou, X., Su, J., Fan, H., Yu, A., Liu, W., Deng, Y., Manzanedo, R.D., Fonti, P., 2019. Physiological and growth responses to increasing drought of an endangered tree species in Southwest China. Forests 10, 514.